

## Triangular Microstrip Antenna for Circularly-Polarized Synthetic Aperture Radar Sensor Application

Muhammad Fauzan Edy Purnomo<sup>1</sup>, Akio Kitagawa<sup>2</sup>

<sup>1,2</sup>Electrical Engineering and Computer Science, Kanazawa University  
Kakuma-machi, Kanazawa, Ishikawa 920-1192, Japan

<sup>1</sup>Electrical Engineering Department, Faculty of Engineering, Brawijaya University, Indonesia  
Jalan MT Haryono 167 Malang 65145 Indonesia, telp/fax: +62 341 554166/551430

---

### Article Info

#### Article history:

Received May 30, 2018

Revised Jun 1, 2018

Accepted Jun 15, 2018

---

#### Keywords:

Basic construction

CP-SAR

LHCP and RHCP

Modified lossless T-junction  
power divider

Triangular microstrip antennas

---

### ABSTRACT

In this paper, we obtain the basic construction of triangular microstrip antennas based on the analysis of the single patch and array two patches. This construction use the basic corporate feeding-line with modified lossless T-junction power divider for Circularly Polarized-Synthetic Aperture Radar (CP-SAR) sensor embedded on airspace with compact, small, and simple configuration. The design of Circular Polarization (CP) is realized by truncating the whole three tips and adjusted the parameters of antennas at the resonant frequency,  $f = 1.25$  GHz. The equations for reciprocal, lossless, and matched of the modified lossless T-junction power divider are also described. The result of characteristic performance and S-parameter for the single patch both Left-Hand Circular Polarization (LHCP) and Right-Hand Circular Polarization (RHCP) at the resonant frequency show consecutively 7.15 dBic and 7.16 dBic of gain, 0.12 dB and 0.11 dB of axial ratio, -26.75 dB and -26.72 dB of S-parameter. For array two patches, the result of gain, axial ratio, and S-parameter both of LHCP and RHCP are 7.63 dBic, 7.62 dBic, 2.68 dB, 2.74 dB, -19.43 dB, and -19.40 dB, respectively. The modified lossless T-junction power divider both for LHCP and RHCP are capable of being reciprocal, matched, and lossless at all ports.

*Copyright © 2018 Institute of Advanced Engineering and Science.  
All rights reserved.*

---

### Corresponding Author:

Muhammad Fauzan Edy Purnomo,  
Electrical Engineering and Computer Science,  
Kanazawa University,  
Kakuma-machi, Kanazawa, Ishikawa 920-1192, Japan.  
Email: purnomo@stu.kanazawa-u.ac.jp

---

## 1. INTRODUCTION

One of an active sensor for the remote sensing application in the microwave band is Synthetic Aperture Radar (SAR). An object or phenomenon can be observed without touching it by this application. Also, it helps human being related to the area of observation, such as surveillance, disaster mitigation, mapping, land, air, and ocean. SAR systems can operate at some different bands and polarizations. The most common band-frequency is C-band which has an approximately 5 cm wavelength. It is used on Radarsat and Envisat systems. S-band ( $\lambda \approx 10$  cm) and L-band ( $\lambda \approx 20$  cm) are also common [1]. Because of the longer wavelength, it penetrates surfaces better. Then, it is useful for sea ice, soil moisture, and vegetation applications where the surface penetration is desirable.

Because of the use of Circularly Polarized-Synthetic Aperture Radar (CP-SAR) sensor, the full characteristic of backscattered SAR signal can pass through the random object. If we compare CP-SAR with the linear polarization SAR sensor, then a great amount of information about the image target will be occurred [2], [3]. Each antenna can generate a wave that yields a Circular Polarization (CP). The technique to achieve CP can be easily obtained namely by exactly adjusting the element parameters, determining locus

feed, and designing corporate feeding-line [4]-[6]. In the simulation of the triangular microstrip antenna, the significant variation performances are also affected by the shaping of feeding and their position toward the radiating patches [7]-[10].

This paper presents the triangular microstrip antenna for CP-SAR sensor application. The study involved the development of the single and array 2 x 1 patches antennas fundamentally construct to mold a substantial planar array using proximity coupled feed. It is because the right pattern of basic construction determines the superiority of the designed array antenna using corporate feeding-line [11]-[14]. Results obtained from the study revealed that S-parameter, frequency characteristic, input impedance, radiation pattern, and antenna efficiency both of the single and array 2 x 1 patches antennas. Also, the study expressed that the modified lossless T-junction power divider 2 x 1 configuration both for Left-Hand Circular Polarization (LHCP) and Right-Hand Circular Polarization (RHCP) are capable of being reciprocal, matched, and lossless at all ports.

## 2. RESEARCH METHOD

In this investigation, we only perform and discuss the result of the numerical simulation related to the microstrip antenna. In particular, the analysis focuses on the study of triangular microstrip antennas both LHCP and RHCP for a single patch and array 2 x 1 patches. Also, we analyze the modified lossless T-junction power divider for CP-SAR sensor embedded in airspace with compact, small, and simple configuration. In this case, the array antennas use the two patches as a transmitter,  $T_x$ , and receiver,  $R_x$  [7], [8]. Table 1 shows the specification for CP-SAR system, which influence the specification of the L-Band CP-SAR airspace antenna [9].

We choose the Method of Moments (MoM) for this numerical analysis to make the fast calculation. This method discretizes the representative signal in the integral form into a discrete quantity and then convert to shape a matrix Equation which can be solved. This discretization can be considered as dividing the antenna surface into some small elements. Furthermore, the current distribution, the S-parameter, the radiation pattern, and the other parameters of interest can be obtained. We use the software of Computer Simulation Technology (CST) version 2016 from corporate company CST STUDIO SUITE [15]. According to the software characteristics, the dielectric substrate and the ground plane are considered to be infinite. In this case, we set them to become finite.

Table 1. The Specification for CP-SAR System

No	Parameter	Specification CP-SAR System
1.	Frequency (GHz)	L-band: 1.25-1.27 GHz; S-band: 2.5-2.9 GHz
2.	Pulse Band Wide (MHz)	10 - 233.31
3.	Axial Ratio (dB)	$\leq 3$
4.	Antenna Efficiency (%)	$> 80$
5.	Gain Antenna (dBic)	10 - 36.6
6.	Azimuth Beamwidth ( $^\circ$ )	$\geq 1.08$
7.	Range Beamwidth ( $^\circ$ )	$\geq 2.16$
8.	Antenna Size (m)	2 x 4
9.	Polarization ( $T_x/R_x$ )	LHCP + RHCP

### 2.1. The LHCP and RHCP Single Patch Antennas Configuration

Figure 1 shows the configuration of LHCP and RHCP single patch antennas design. The equilateral triangular patch has a length,  $a + t + h = p + 2t$  and a conventional substrate,  $\epsilon_r = 2.17$  and  $\delta = 0.0005$ . The antenna is fed by proximity couple located on the left side for LHCP and on the right side for RHCP. The length of parameters in the design of LHCP and RHCP antennas are the same size for  $a, p, h, t, w1, w2$ , etc. In this case, the truncated-tip of  $t = 1.5008$  mm and  $h = 7.64$  mm for smooth performance of the results. If  $t > h$ , then LHCP and RHCP are obtained when the proximity coupled feed is located on the right and the left side of the equilateral triangular patch antenna, respectively. Otherwise, if  $t < h$ , in the same manner, that LHCP and RHCP occur as the proximity coupled feed is consecutively lied on the left and the right side. As well, the function of  $t$  serve as switching to change the variation of polarization, if the proximity coupled feed is located on the same place (for example, the proximity coupled feed locus in the right side,  $t < h$ , RHCP will be achieved on that place). If  $t = h$ , then both of the antennas do not have CP and only obtain a linear polarization [9].

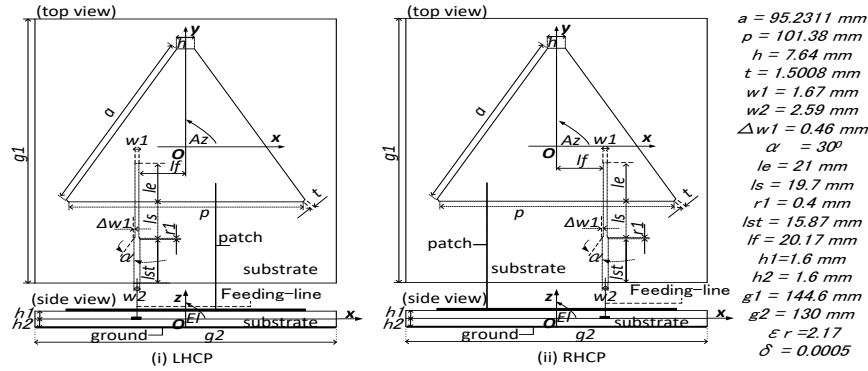


Figure 1. Configuration of the LHCP and RHCP single patch antennas

**2.2. The LHCP and RHCP Modified Lossless T-junction Power Divider 2 □ 1 Configuration**

The power divider is a network with one input port and  $N$  output ports. The input power at the input port will be divided by the number of the output ports that yield the same output power at each output port. The incident waves and the reflected waves are related to input power and output power at the input port and the output ports. Then, the  $S$ -matrix regarding incident waves ( $a$ ) and reflected waves ( $b$ ) can be written as [16]-[18]

$$[b] = [S][a] \text{ or } \begin{bmatrix} b_1 \\ b_2 \\ \vdots \\ b_N \end{bmatrix} = \begin{bmatrix} S_{11} & S_{12} & \dots & S_{1N} \\ S_{21} & S_{22} & \dots & S_{2N} \\ \vdots & \vdots & \ddots & \vdots \\ S_{N1} & S_{N2} & \dots & S_{NN} \end{bmatrix} \begin{bmatrix} a_1 \\ a_2 \\ \vdots \\ a_N \end{bmatrix} \tag{1}$$

The general Equation for an element of the  $S$ -matrix can be defined as

$$S_{ij} = \left. \frac{b_i}{a_j} \right|_{a_k=0, k \neq j} \tag{2}$$

In principle, an incident wave drives port  $j$  and a reflected wave exits port  $i$ , where the ratio of the reflected wave to incident wave provides the  $S$ -matrix element  $S_{ij}$ . Additionally, the incident waves on all ports other than port  $j$  are set equal to zero. A vector network analyzer is typically used to measure these parameters.

One common characteristic found in power dividers is reciprocity. A reciprocal device is the one in which the transmitted power between two ports of the device is the same regardless of the propagation direction through the device. For a reciprocal device [16]-[18], we have

$$[S] = [S]^T \text{ or } S_{ij} = S_{ji} ; \text{ for all } i \text{ and } j \tag{3}$$

Another property of the  $S$ -matrix is how much loss that can be attributed to the device. Ideally, a lossless power divider will be used in a system. However, the only low-loss divider is physically realizable. It has been shown, mainly by Pozar, that if the  $S$ -matrix of the device is unitary, then the device is lossless, as follow [16-18]

$$[S]^T [S]^* = [I] \text{ or } [S^*]^T [S] = [I] \tag{4}$$

where  $[I]$  is the identity matrix, the superscript  $T$  represents the its transpose, and the superscript asterisk (\*) represents the its conjugate.

For three ports power divider, isolation between output ports, port 2 and port 3 (see Figure. 2), is prominent for reducing cross-talk that can be caused by coupling between the ports. By definition, a -3 dB power divider is an ideal passive lossless reciprocal three ports device that divides power equally in magnitude and phase. The  $S$ -parameter matrix related to this device is:

$$[S] = \begin{bmatrix} S_{11} & S_{12} & S_{13} \\ S_{21} & S_{22} & S_{23} \\ S_{31} & S_{32} & S_{33} \end{bmatrix} \tag{5}$$

According to the matrix in (5), the condition for a lossless network is given by Equation (4). Also, the situation for a reciprocal network is described in Equation (3). Then, the state for coefficient reflection load ( $\Gamma_L$ ) is

$$\Gamma_L = 1 - |S_{ij}|^2 = \frac{\text{reflection wave}}{\text{incident wave}}; 0 \leq \Gamma_L \leq 1; i, j = 1, 2, 3 \tag{6}$$

If  $\Gamma_L = 1[0^\circ$ , then it occurs an open circuit condition. If  $\Gamma_L = 1[180^\circ$ , this is a short circuit condition. If  $\Gamma_L = 0$ , then this is a matched load circuit condition. Since all the three ports of this power divider are matched, then  $S_{ii} = 0$ . The modified  $S$ -matrix for matched load condition is

$$[S] = \begin{bmatrix} 0 & S_{12} & S_{13} \\ S_{21} & 0 & S_{23} \\ S_{31} & S_{32} & 0 \end{bmatrix} \tag{7}$$

In the  $S$ -matrix, the elements  $S_{23}$  and  $S_{32}$  are associated with the isolation between the output ports. These correspond to signals entering port 2 and exiting port 3, and vice versa. When the magnitudes of these elements are small, high isolation is achieved between the ports. For the lossless condition to be true, the matrix in Equation (7) must be unitary and satisfy.

$$|S_{12}|^2 + |S_{13}|^2 = 1 \tag{8}$$

$$|S_{12}|^2 + |S_{23}|^2 = 1 \tag{9}$$

$$|S_{13}|^2 + |S_{23}|^2 = 1 \tag{10}$$

$$S_{13}^* S_{23} = 0 \tag{11}$$

$$S_{23}^* S_{12} = 0 \tag{12}$$

$$S_{12}^* S_{13} = 0 \tag{13}$$

This lossless form means that two of the elements  $S_{12}$ ,  $S_{13}$ , and  $S_{23}$  must be equal to zero to satisfy Equations (11) – (13). For the sake of clarity of this analysis,  $S_{12}$  and  $S_{13}$  set equal to zero. However, it is obvious that by setting  $S_{12}$  and  $S_{13}$  equal to zero, Equation (8) is not satisfied. Consequently, when two of the elements  $S_{12}$ ,  $S_{13}$ , and  $S_{23}$  are equal to zero, one of the Equations (8)-(10) will not be satisfied. Thus a matched, reciprocal, lossless of three ports network becomes impossible to be realized [16-18].

**2.3. The LHCP and RHCP Array Two Patches Antennas Using the Modified Lossless T- junction Power Divider 2 x 1 Configuration**

Figure 2 show the configuration of triangular array antenna both LHCP and RHCP include the two radiating patches fed by corporate feeding-line with identical path lengths from the input port to output ports and their parameters. The aim of designed the corporate feeding-line is to acquire a tapered and in-phase output current distribution [10], [14]. The parameter sizes of each patch (patch 1 and patch 2) are the same, namely the length of triangle side,  $a = 95.2311$  mm and  $p = 101.38$  mm, the length of perturbation segment,  $h = 7.64$  mm and  $t = 1.5008$  mm. Furthermore, the corporate feeding-line has one node of T-junction. This node has a function to distribute the current with the power of around 30 dBm and to reach  $2 \times 1$  patches having the same length from the input port to radiating patches or output ports around  $9.32\lambda$  or  $379.315$  mm.

To design the microstrip patch antenna, we choose a suitable dielectric constant with appropriate thickness and loss tangent. A low value of the dielectric constant will increase the fringing field at the patch periphery. A thicker substrate will increase the radiation power, reduce conductor loss, and improve impedance bandwidth. A high loss tangent rises dielectric loss and then reduces antenna efficiency [11-13]. In this paper, Nippon Pillar Packing (NPC) H220A is chosen as the antenna substrate. It has a conventional substrate with dielectric constant ( $\epsilon_r$ ), and loss tangent ( $\delta$ ) are 2.17 and 0.0005, respectively. Moreover, the total substrate thickness of both LHCP and RHCP antennas is 3.2 mm.

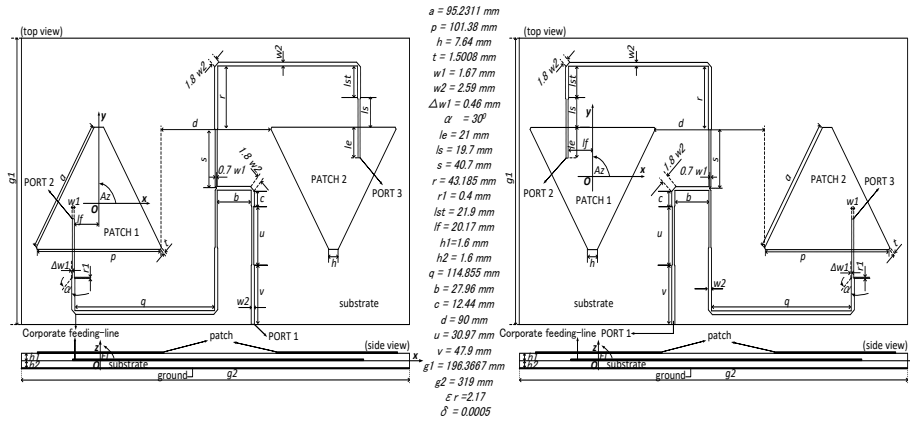


Figure 2. Configuration of LHCP and RHCP array antennas using power divider 2 × 1

### 3. RESULTS AND ANALYSIS

#### 3.1. The LHCP and RHCP Single Patch Antennas

In general, the discussion of the single patch antenna is limited only in the electric field. Especially for far-field or called as radiation characteristic, the elevation plane is mostly described rather than azimuth plane. As we know that the angle  $\phi$  denote x-y or azimuth or magnetic field plane (moves from  $0^\circ$  in positive x-axes and rotates  $360^\circ$ ) and  $\theta$  indicate elevation or electric field plane (stir from  $0^\circ$  or elevation angle,  $EI = 90^\circ$  in positive z-axes to negative z-axes precisely  $180^\circ$  or  $EI = -90^\circ$ ).

Figure 3 shows that the frequency characteristic is not different for both LHCP and RHCP, at the resonant frequency,  $f = 1.25$  GHz, i.e. 7.15 dBic and 7.16 dBic of gain, 0.12 dB and 0.11 dB of the axial ratio (Ar), respectively. Moreover, the Ar-3 dB bandwidth both for LHCP and RHCP are the same around 14 MHz (1.12%). Figure 4 depicts the relationship between the S-parameter and frequency for simulation of Tx/Rx antenna. From this figure, it can be seen the values of reflection coefficient (S-11) at the resonant frequency for LHCP = -26.75 dB and for RHCP = -26.72 dB. In addition, the S-11 bandwidth both LHCP and RHCP are similar around 34 MHz (2.72%). Figure 5 describes that the input impedances of triangular array antennas at the resonant frequency are  $50.54 \Omega$  (LHCP) and  $50.53 \Omega$  (RHCP), close to  $50 \Omega$ . The reactance parts of these antennas are  $4.58 \Omega$  (LHCP) and  $4.60 \Omega$  (RHCP), then it looks inductive and relative close to  $0 \Omega$ .

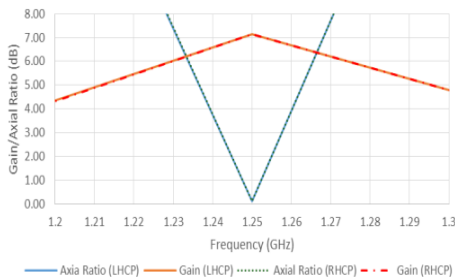


Figure 3. Frequency characteristic

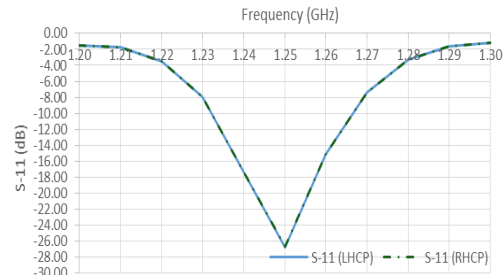


Figure 4. S-parameter

Figure 5 depict the relationship between gain-Ar and elevation angle at azimuth angle,  $Az = 0^\circ$ . At the elevation,  $EI = 90^\circ$  the maximum gain of LHCP and RHCP antennas are about 7.15 dBic and 7.16 dBic, respectively. Also, they are a little bit different for Ar, about 0.12 dB and 0.11 dB for each LHCP and RHCP antenna at  $EI = 90^\circ$ . Moreover, 3 dB-Ar beamwidth for simulation at  $Az = 0^\circ$  both of LHCP and RHCP are similar about  $105^\circ$ . It is satisfied the targeted range/elevation beamwidth of  $\geq 2.16^\circ$  at Table 1 for better resolution of CP-SAR airspace antenna.

Figure 6-7 describes the characteristic of azimuth plane generated by the LHCP and RHCP triangular microstrip patch antennas using proximity coupled feed in the area of  $EI = 90^\circ$  or  $\theta = 0^\circ$  at the resonant frequency. From this figure, we can see that the values of 3 dB-Ar beamwidth cover perfectly the whole of  $360^\circ$ . This result exhibit that the targeted azimuth beamwidth of  $\geq 1.08^\circ$  obtains the resolution of

CP-SAR using airspace. Figure 8 shows the antenna efficiency that is meant the radiation efficiency about 91.39% for LHCP and 91.53% for RHCP antennas on a target frequency of 1.25 GHz. This result denotes that the targeted antenna efficiency of 80% is acquired for CP-SAR using airspace.

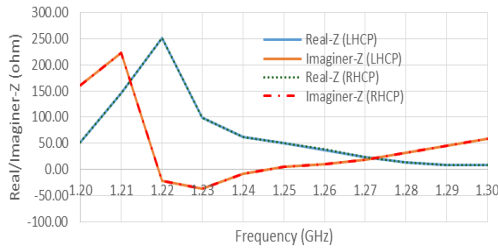


Figure 5. Input impedance

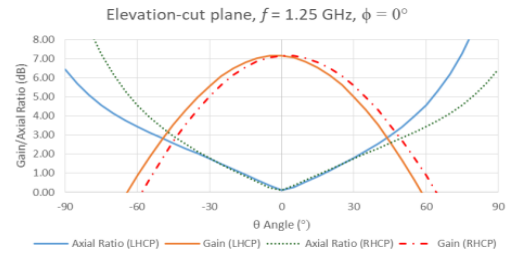


Figure 6. The x-z plane

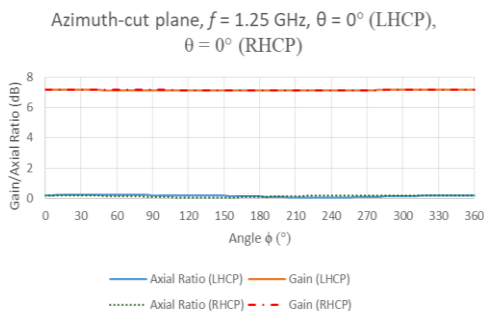


Figure 7. The x-y plane

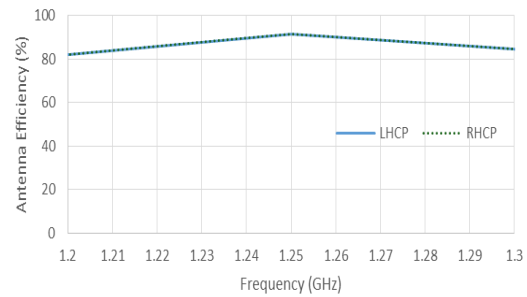


Figure 8. Antenna efficiency

### 3.2. The LHCP and RHCP Modified Lossless T-junction Power Divider 2 x 1

The real and imaginary parts of  $S$ -matrix when the radiating patches are excluded and only the modified lossless T-junction power divider  $2 \times 1$  both LHCP and RHCP (Figure. 2) at  $f = 1.25$  GHz taken from CST software are shown in Equation (14) and (15), respectively. We define that  $[S]_{LHCP}^T$  and  $[S]_{LHCP}^*$  are transpose and a conjugate matrix of (14), respectively. Also, we notice that  $[S]_{RHCP}^T$  and  $[S]_{RHCP}^*$  are consecutively transpose and a conjugate matrix of (15).

$$[S]_{LHCP} = \begin{bmatrix} 0.04 + j0.16 & 0.44 - j0.53 & 0.43 - j0.54 \\ 0.44 - j0.53 & -0.39 - j0.08 & 0.55 + j0.09 \\ 0.43 - j0.54 & 0.55 + j0.09 & -0.38 - j0.07 \end{bmatrix} \quad (14)$$

$$[S]_{RHCP} = \begin{bmatrix} 0.04 + j0.16 & 0.43 - j0.54 & 0.44 - j0.53 \\ 0.43 - j0.54 & -0.38 - j0.07 & 0.55 + j0.09 \\ 0.44 - j0.53 & 0.55 + j0.09 & -0.39 - j0.08 \end{bmatrix} \quad (15)$$

For reciprocity, they are clear for both LHCP and RHCP, i.e.  $[S]_{LHCP} = [S]_{LHCP}^T$  and  $[S]_{RHCP} = [S]_{RHCP}^T$ . The matched ports of the divider set for LHCP  $S_{11} = 0.04 + j0.16$ ,  $S_{22} = -0.39 - j0.08$ , and  $S_{33} = -0.38 - j0.07$  and for RHCP  $S_{11} = 0.04 + j0.16$ ,  $S_{22} = -0.38 - j0.07$ , and  $S_{33} = -0.39 - j0.08$  are relatively close to zero. It means that only little bit of the incident waves on the matched port will be reflected or not exit the ports. Thus, the reflected waves at the ports will close to zero. We get that the both LHCP and RHCP are almost the lossless of the power divider,  $[S]^T[S]^* = [I]$  or  $[S]^*[S]^T = [I]$ , as seen in (16) and (17).

$$[S]^T[S]^*_{LHCP} = \begin{bmatrix} 0.9782 & -0.0085 - j0.0022 & -0.0005 - j0.0054 \\ -0.0085 + j0.0022 & 0.9436 & 0.0384 + j0.0051 \\ -0.0005 + j0.0054 & 0.0384 - j0.0051 & 0.9364 \end{bmatrix} \approx \begin{bmatrix} 1 & 0 & 0 \\ 0 & 1 & 0 \\ 0 & 0 & 1 \end{bmatrix} \quad (16)$$

$$[S]^T[S]^*_{RHCP} = \begin{bmatrix} 0.9782 & -0.0005 - j0.0054 & -0.0085 - j0.0022 \\ -0.0005 + j0.0054 & 0.9364 & 0.0384 - j0.0051 \\ -0.0085 + j0.0022 & 0.0384 + j0.0051 & 0.9436 \end{bmatrix} \approx \begin{bmatrix} 1 & 0 & 0 \\ 0 & 1 & 0 \\ 0 & 0 & 1 \end{bmatrix} \quad (17)$$

### 3.3. The LHCP and RHCP Array Two Patches Antennas Using the Modified Lossless T-junction Power Divider 2 x 1

When the radiating patches and the modified lossless T-junction power divider  $2 \times 1$  network are operated in the CST software, then the results show in Figure 9 to Figure 14 for simulation of triangular microstrip array  $2 \times 1$  both of LHCP and RHCP antennas, in the case of frequency characteristic, S-parameter, input impedance, radiation pattern, and antenna efficiency.

Figure 9 shows that the values of gain and axial ratio ( $Ar$ ) for simulation of triangular array antennas in the direction of  $\theta = -29^\circ$  for LHCP and  $\theta = 30^\circ$  for RHCP at the resonant frequency,  $f = 1.25$  GHz, are about 7.63 dBic, 2.68 dB, 7.62 dBic, and 2.74 dB, respectively. In addition, the  $Ar$ -3 dB bandwidth both for LHCP and RHCP are roughly equal 4 MHz (0.32%). Figure 10 shows the relationship between the reflection coefficient (S-11) and the frequency for the simulation  $T_x/R_x$  triangular array antennas. Moreover, the S-11 values at the resonant frequency for LHCP = -19.43 dB and for RHCP = -19.40 dB. While the S-11 bandwidth both LHCP and RHCP are similar around 37 MHz (2.96%). Figure 11 depicts the input impedance characteristic of the triangular array  $2 \times 1$  antennas both LHCP and RHCP that consecutively the real parts of simulation at the resonant frequency are  $40.73 \Omega$  and  $40.72 \Omega$ , relative close to  $50 \Omega$ . The reactance parts of these antennas are  $-1.73 \Omega$  (LHCP) and  $-1.84 \Omega$  (RHCP), then it looks capacitive and close to  $0 \Omega$ . In the feed network, the length from the input port to output ports must be fixed at  $l \lambda/4$  ( $l = 1, 3, 5$ , etc.) to achieve the optimal current intensity [2], [10]. In this work, we use  $l = 9$ .

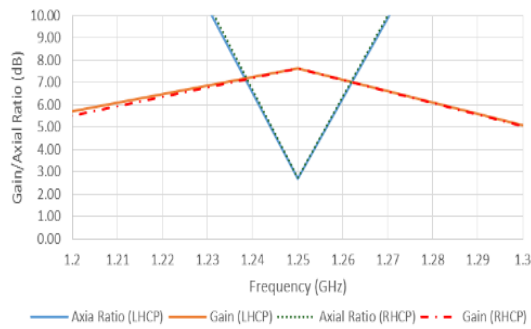


Figure 9. Frequency characteristic of array antenna

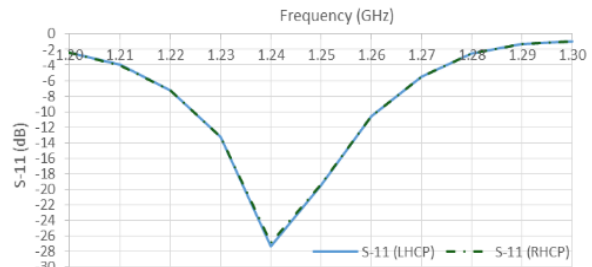


Figure 10. S-parameter of array antenna

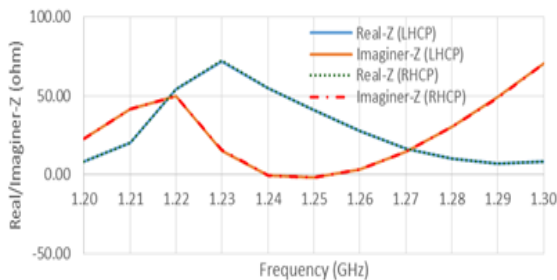


Figure 11. Input impedance of array antenna

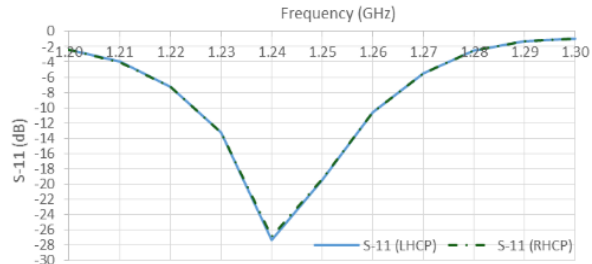


Figure 12. The  $x$ - $z$  plane of array antenna

Figure 13 describes the azimuth plane in the area of  $\theta = -29^\circ$  for LHCP and  $\theta = 30^\circ$  for RHCP at 1.25 GHz. The major values of 3 dB- $Ar$  beamwidth of LHCP are about  $57^\circ$  from  $\phi = 308^\circ$  to  $\phi = 5^\circ$  and around  $50^\circ$  from  $\phi = 130^\circ$  to  $\phi = 180^\circ$ . While for RHCP are roughly  $55^\circ$  from  $\phi = 0^\circ$  to  $\phi = 55^\circ$  and approximately  $45^\circ$  from  $\phi = 180^\circ$  to  $\phi = 225^\circ$ . Figure 14 shows the antenna efficiency about 87.25% for LHCP and 87.08% for RHCP antennas on a target frequency of 1.25 GHz. These results exhibit that the targeted azimuth beamwidth  $\geq 1.08^\circ$  and the targeted antenna efficiency of 80% obtain the resolution of CP-SAR.

We can conclude that the graph both of LHCP and RHCP coincide with each other, especially for frequency characteristic, S-parameter, input impedance, elevation-cut plane, and antenna efficiency. It means that the good results are attained by LHCP and RHCP triangular microstrip antennas using the same

parameters. Only one of their feeding is flipped toward y-axis for a single patch and also reversed toward y-axis together with the radiating patches rotated  $180^\circ$  in the same place for array two patches. But for azimuth-cut plane are relatively different because the maximum values of gain and the minimum values of axial ratio are achieved with different angles  $\theta$  for each type, LHCP ( $\theta = -29^\circ$ ) and RHCP ( $\theta = 30^\circ$ ).

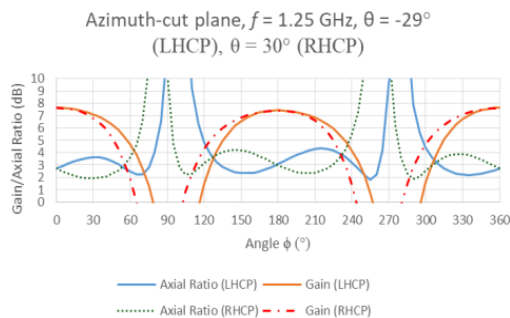


Figure 13. The  $x$ - $y$  plane of array antenna

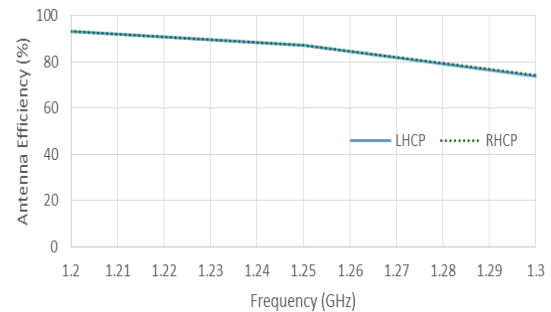


Figure 14. Antenna efficiency of array antenna

#### 4. CONCLUSION

The analysis performances of triangular microstrip both single patch and array two patches antennas using modified lossless T-junction power divider at the L-band frequency with low power ( $\approx 30$  dBm) for CP-SAR airspace have been studied. The performance results both LHCP and RHCP are as follow: (i) For the single patch, the  $Ar$ -3 dB bandwidth both for LHCP and RHCP are the same around 14 MHz (1.12%). The 3 dB- $Ar$  elevation beamwidth for simulation at  $A_z = 0^\circ$  both of LHCP and RHCP are about  $105^\circ$ . The 3 dB- $Ar$  azimuth beamwidth cover perfectly the whole of  $360^\circ$ . The antenna efficiency is about 91.39% for LHCP and 91.53% for RHCP antennas on a target frequency of 1.25 GHz. (ii) For array two patches, the  $Ar$ -3 dB bandwidth both for LHCP and RHCP are roughly equal 4 MHz (0.32%). The average values of 3 dB- $Ar$  elevation beamwidth are  $35^\circ$  ( $A_z = 0^\circ$  and  $A_z = 180^\circ$ ) for LHCP and  $42^\circ$  ( $A_z = 0^\circ$  and  $A_z = 180^\circ$ ) for RHCP at boresight. The key values of the average 3 dB- $Ar$  azimuth beamwidth of LHCP and RHCP at boresight are consecutively about  $53.5^\circ$  and  $50^\circ$ . The antenna efficiency is about 87.25% for LHCP and 87.08% for RHCP antennas on a target frequency of 1.25 GHz. (iii) The modified lossless T-junction power divider both for LHCP and RHCP are capable of being reciprocal, matched, and lossless at all ports. These results temporarily meet the application of CP-SAR airspace.

#### ACKNOWLEDGEMENTS

The authors would like to express their gratitude to the Microelectronic Research Laboratory (MeRL), Electrical Engineering and Computer Science, Graduate School of Natural Science and Technology, Kanazawa University, Japan for the support of expense and the facilities to collect the data in this research. Special thanks to Ministry of Finance, Indonesia Endowment Fund for Education (LPDP) and Ministry of Research, Technology and Higher Education (RISTEKDIKTI) for the support of scholarship. Also thanks to Brawijaya University, especially Department of Electrical Engineering, Faculty of Engineering for the support in my research.

#### REFERENCES

- [1] Purnomo MFE, Sumantyo JTS. *Design Circularly Polarized of Equilateral Triangular Hole Antenna for SAR (Synthetic Aperture Radar)*. IEICE Technical Report, ISSN: 0913-5685. October 17-19, 2011; Vol. 111; No. 239.
- [2] Yohandri, Wissan V, Firmansyah I, Akbar Rizki P, Sumantyo JTS, Kuze H. *Development of Circularly Polarized Array Antenna for Synthetic Aperture Radar Sensor Installed on UAV*. Progress In Electromagnetics Research C. 2011; Vol. 19: 119 – 133.
- [3] Baharuddin M, Wissan V, Sumantyo JTS, Kuze H. *Equilateral Microstrip Antenna for Circularly-Polarized Synthetic Aperture Radar*. Progress In Electromagnetic Research C. 2009; Vol. 8: 107 – 120.
- [4] Purnomo MFE, Suyono H, Mudjirahardjo P, Hasanah RN. *Analysis Performance of Singly-fed Circularly Polarized Microstrip Antenna for Wireless Communication*. Jurnal TEKNOLOGI, e-ISSN: 2180-3722. May 2016; Vol. 78; No. 5 – 9.
- [5] Tang CL, Lu JH, Wong KL. *Circularly Polarized Equilateral-Triangular Microstrip Antenna with Truncated tip*. Electron. Letter. June 1998; Vol. 34: 1227 – 1228.

- [6] Purnomo MFE, Rahmadwati, Suyono H, Yuwono R, Sumantyo JTS. *Development L-Band Antenna with Low Power for Circularly Polarized-Synthetic Aperture Radar (CP-SAR) Application on Unmanned Aerial Vehicle (UAV)*. Proceedings of The 7th Indonesia Japan Joint Scientific Symposium. The 24th CEReS International Symposium. The 4th Symposium on Microsatellite for Remote Sensing (SOMIRES 2016). The 1st Symposium on Innovative Microwave Remote Sensing. Keyaki Convention Hall. ISSN: 978-4-901404-15-0. 20-24 November 2016; 392 – 403.
- [7] Sumantyo JTS, Ito K, Takahashi M. *Dual-Band Circularly Polarized Equilateral Triangular-Patch Array Antenna for Mobile Satellite Communications*. IEEE Transactions on Antennas and Propagation, November 2005; vol.53; No.11.
- [8] Purnomo MFE, Pramono SH, Pamungkas MA, Taufik. *Study of The Effect of Air-gap on Array Microstrip Antenna Performances for Mobile Satellite Communications*. ARPN Journal of Engineering and Applied Sciences ISSN: 1819-6608. November 2015; Vol.10; No.20.
- [9] Purnomo MFE, Kitagawa A. *Analysis Performance of Triangle Microstrip Antenna for Basic Construction of Circularly Polarized-Synthetic Aperture Radar Application*. Jurnal TEKNOLOGI, e-ISSN: 2180-3722. March 2018; Vol. 80; No. 2. DOI: <https://doi.org/10.11113/jt.v80.11119>.
- [10] Purnomo MFE, Kitagawa A. *Development of Sixteen Elements of Microstrip Triangular Array Antenna for Circularly Polarized-Synthetic Aperture Radar Sensor Application*. J. Fundam. Appl. Sci., 2018, 10(5S), 535 – 550.
- [11] Purnomo MFE, Setyawati O, Suyono H, Hasanah RN, Mudjirahardjo P, Rahmadwati. *The Analysis of Stub on Coplanar-fed of Single and Array Microstrip Antenna for Mobile Satellite Communication*. International Journal on Advanced Science, Engineering and Information Technology, ISSN: 2088-5334. 2017; Vol.7; No. 5: 1927 – 1933. DOI: 10.18517/ijaseit.7.5.3676.
- [12] Salihah S, Jamaluddin MH, Selvaraju R, Hafiz MN. *A MIMO H-shape Dielectric Resonator Antenna for 4G Applications*. Indonesian Journal of Electrical Engineering and Computer Science, ISSN: 2502-4752. May 2018; Vol. 10; No. 2: 648 – 653. DOI: 10.11591/ijeecs.v10.i2.pp648-653.
- [13] Shahadan NH, Kamarudin MR, Jamaluddin MH, Yamada Y. *Higher-order Mode Rectangular Dielectric Resonator Antenna for 5G Applications*. Indonesian Journal of Electrical Engineering and Computer Science. March 2017; Vol. 5; No. 3: 584 – 592. DOI: 10.11591/ijeecs.v5.i3.pp584-592.
- [14] Gupta KC, Garg R, Bahl I, Bhartia P. *Microstrip Lines and Slotlines*. Artech House, Inc. Second Edition ISBN: 0-89006-766-X. 1996.
- [15] CST STUDIO SUITE 2016. *Microwave - radio frequency – optical*. Copyright © 1998 – 2016 CST AG, Release version 2016. November 11, 2016.
- [16] Pozar D. *Microwave Engineering*. John Wiley & Sons Inc. 3rd ed. Hoboken, New Jersey, 2005; 308 – 361.
- [17] Grebennikov A. *RF and Microwave Transmitter Design*. John Wiley & Sons Inc. Hoboken, New Jersey, 2011.
- [18] Chang K. *Encyclopedia of RF and Microwave Engineering*. John Wiley & Sons Inc. Hoboken, New Jersey, 2005.